Water Research, Volume 206, November 2021, Article number 117779
DOI:10.1016/j.watres.2021.117779

Development and calibration of a new mathematical model for the description of an ion-exchange process for ammonia removal in the presence of competing ions

I. Lizarralde[1], S. Guida[2], J. Canellas[3], B. Jefferson[2], P. Grau[1] and A. Soares[2]

[1] Ceit and Tecnun (University of Navarra) Manuel de Lardizábal 15, 20018 San Sebastián, Spain
(E-mail:*ilizarralde@tecnun.es; pgrau@tecnun.es*)
[2]Cranfield University, School of Water Sciences, Cranfield University, Cranfield, Bedfordshire, MK43 0AL UK
(Email: *Samuela.Guida@Cranfield.ac.uk; B.Jefferson@cranfield.ac.uk;* a.soares@cranfield.ac.uk)
[3]Department of Chemistry, Biology and Environmental Engineering, School of Engineering, Autonomous University of Barcelona, 08193 Bellaterra, Barcelona, Spain
(Email: judit.canellas@uab.cat)

Abstract

Ammonia ion removal and recovery via an ion-exchange process using zeolites is a promising alternative to traditional biological treatments. The analysis of its efficiency is not straightforward as it depends on various factors, such as the cation exchange capacity of the zeolite, amount of zeolite available, initial ammonia concentration, contact time, ammonia speciation depending on pH or the presence of competing ions. Mathematical modelling and simulation tools are very useful to analyse the effect of different operational conditions on the efficiency and optimal operation of the process. This paper experimentally analyses the effect that the presence of competing ions has on the efficiency of ammonia removal. This experimental work has shown a reduction of around 21% of ammonia removal efficiency in the presence of competing ions. The main contribution of this paper is the development new mathematical model able to describe the ion-exchange process in the presence of competing ions. The mathematical model developed is able to analyse the performance of the IEX process under different empty bed contact times, influent loads, pH and concentrations of competing ions. The capability of the model to reproduce real data has been proven comparing the experimental and simulation results. Finally, an exploration by simulation has been undertaken to show the potential of the mathematical model developed.

Keywords
Ammonia recovery; Ion-Exchange process; Mathematical modelling; Resource-recovery, NET-ZERO targets

1. INTRODUCTION

The implementation of more restrictive water quality regulations along with the introduction of targets to reduce greenhouse gases emissions and the scarcity of valuable products is empowering a

fresh discussion on the most appropriate technologies for wastewater treatment. The most apposite of which relates the ammonia ion (NH_4^+) due to it connection to both the emerging hydrogen economy and the net zero carbon agenda. Traditionally, nitrogen is removed from wastewater using biological nitrification-denitrification processes, which are very sensitive to the presence of toxic compounds, operational pH, variations in temperature and availability of oxygen (Henze *et al.,* 2008). The main disadvantages of these biological processes are the high energy consumption required to aerate the system (Tchobanoglous *et al.,* 2003; Olsson *et al.,* 2013) and the fact that during the nitrification-denitrification process, NH_4^+ is transformed rather than being captured with a proportion transforms into nitrous oxide, which is a powerful greenhouse gas (Soares, 2020). In this context, IEX processes using zeolites offer a promising alternative to biological treatment for NH_4^+ removal, guaranteeing low energy consumptions and minimisation of nitrous oxide emission (Wang *et al.,* 2006; Sancho *et al.,* 2017; Huang *et al.,* 2020). However, one of the main concerns when using IEX processes for ammonia removal is the disposal of the associated brines. This has led to increasing research into recovery options transforming a potential problem into a resource (Iddya *et al., 2020; Guida et al.,* 2022)

Ion exchange have been applied for the treatment of water and wastewater for heavy metal removal (Kumar *et al.,* 2017); water softening (Flodman and Dvorak, 2012; Comstock and Boyer*,* 2014); removal of natural organic matter (Levchuk *et al.,* 2018) or nutrient removal and recovery in wastewater treatment (Robles *et al.,* 2020).

Zeolites are aluminosilicates with a net negative charge that is neutralized by the presence of cations within its pores. When in contact with wastewater, the NH_4^+ is exchanged with the cations on the zeolite's framework, most commonly potassium (K^+) or sodium (Na^+), which are then released into the water. The prolonged exchange of NH_4^+ in wastewater causes the zeolite to reach saturation and therefore, needs to be regenerated. The regeneration is traditionally accomplished using a concentrated K^+ (or Na^+) brine in order to return the original cations on the zeolite and in return, NH_4^+

65 is released to the regenerant.

66 The efficiency of the IEX process depends on various factors such as the cation exchange capacity of
67 the zeolite, amount of zeolite available, initial NH_4^+ concentration, contact time and the pH through
68 it impact on ammonia speciation (Worch, 2012). A critical aspect in understanding the feasibility of
69 the process in practice is the impact of competing ion as they are known to reduce the effective
70 capacity of the zeolite and its associated cycle time. To illustrate, previous research has suggested a
71 reduction in 30% in capacity when comparing mono component systems to real wastewaters
72 (Thornton *et al.,* 2007; Weatherley and Miladinovic, 2004). In spite of its relevance, there remain a
73 paucity of studies examining the effect of competing ions on the process (Prelot *et al.,* 2018). A key
74 relationship exists between the exchange between NH_4^+ and K^+ cations. Theoretically, the exchange
75 ratio NH_4:K (in meq) is 1:1, and this ratio is important to determine the number of cycles with which
76 the regenerant can be reused without replenishment.

77 Analysing all the factors experimentally is time and resource consuming such that the use of
78 mathematical models and simulation tools can be very useful (Victor-Ortega, *et al.,* 2016) in finding
79 the optimum values for design and operation. In this context, several authors have proposed different
80 models for the description of IEX process with different scope and structures.

81 The most comprehensive mathematical models are the mono component isotherm models such as the
82 Langmiur or Freudlinch models that describe the equilibrium rather than kinetic aspects of the process
83 and are not appropriate to assess competing species. These were initially developed for adsorption of
84 gaseous component but nowadays are widely applied to liquid adsorption or IEX processes (Wang *et*
85 *al.,* 2006; Thornton *et al.,* 2007; Ding and Sartaj, 2015). In order to describe the kinetics and dynamic
86 behaviour of the process, several models have been proposed in literature (Worch, 2012; Trgo *et al.,*
87 2011; Worch, 2008). The main difference between these is the driving force used to describe the
88 process. Among others, the Thomas model (Thomas, 1944) describes the process rate depending on
89 concentration of cations in the solution and the difference between the available sites in the adsorbent

and actual adsorbed cations. The integrated form of this model is one of the most general and widely used model, which is applicable to systems with constant flow rate (Trgo *et al.,* 2011). Alternative models include the film diffusion mass transfer model which considers the difference between the concentration in the bulk solution and the concentration in the external surface in the boundary layer as the driving force of the process (Worch, 2012) and the surface diffusion or the homogeneous diffusion model, where the driving force of the process is the concentration gradient in the solid phase. This model considers variations in time and space and describes the process in a very detailed way, albeit exerting a high computational cost. Hence, a simplified intraparticle diffusion model considering only time variations has been proposed (Worch, 2008).

In addition to the specific limitations, all these models present some common assumptions and simplifications that may limit their predictive capacity. All these models represent the process as functioning by a pure adsorption process, omitting the release of the original cation present on the zeolite into the water, i.e. the IEX process. Another limitation is that these models do not consider the speciation of NH_4^+ and, consequently, the effect of pH on the process is not taken into consideration. This approach can be valid for wastewaters with pH below 8. However, at higher pH values, uncharged NH_3 is also present in water which is not available to exchange. Having a model able to predict this speciation is vital, especially for wastewaters that have pH between 8 and 9, for example when treating industrial effluents. Finally, a further limitation of these models is that they were not conceived nor developed to be analysed in a wastewater treatment plant (WWTP) context, so they present compatibility limitations with other conventional process models making the analysis of novel plant configurations that include the IEX process very difficult. Such wastewater treatment (WWT) process models (ASM 1, ADM1) are based on the definition of a stoichiometric matrix and the process kinetics (Henze *et al.,* 2000; Batstone and Keller, 2002). Accordingly, having a mathematical model that follows this structure for the definition of the IEX process would enable effective comparative analysis of different flowsheets with combinations of traditional WWT processes and

115 IEX technology.

116 Considering the aforementioned limitations, the aim of this study was the definition of a methodology
117 for the development and calibration of a mathematical model to describe an IEX process for NH_4^+
118 removal and recovery in the presence of competing ions such as Ca^{2+}, Mg^{2+} and Na^+ and their
119 interaction with K^+ using zeolite as adsorbent material. This mathematical model is able to analyse
120 the performance of the IEX process under different empty bed contact times, influent loads, pH and
121 concentrations of competing ions. To achieve this, a set of experiments were undertaken to analyse
122 the kinetics of the IEX process and determine the associated mass balances using different types of
123 wastewater. The mathematical model constructed in this paper was calibrated using the experimental
124 data. The calibrated model was then utilised to show the capability of the model in predicting the
125 performance of the continuous operation of the IEX process under different operational conditions.

126 **2. MATERIALS AND METHODS**

127 **2.1 Experimental work**

128 The experimental work was designed with two main objectives: (1) the definition of the process
129 kinetics and (2) the definition of the complete mass balance of the cations present in the water for the
130 IEX process.

131 A synthetic zeolite supplied by Nanochem Pty Ltd. (Australia) was used in these experiments. Batch
132 tests were carried out in triplicate in 1L bottles containing 10 g of zeolite each. The media was pre-
133 treated and conditioned before conducting the experimental cycles. The pre-treatment consisted of
134 two cycles of adsorption and regeneration. The adsorption phase lasted 6 hours and used a solution
135 containing 14.00 mg NH_4^+/L in de-ionised (DI) water using NH_4Cl (purity stated >99%, Fisher
136 Scientific, UK) was used. The regeneration lasted 2 hours and was carried out using a brine containing
137 10%wt K^+ (purity stated >99%, Fisher Scientific, UK).

138 In order to analyse different cations concentrations and consequent competition for exchange sites,
139 five different solutions were used:

(1) A solution containing 12.74 mg NH_4^+/L dissolved in de-ionised (DI) water using NH_4Cl (purity stated >99%, Fisher Scientific, UK). The NH_4^+ concentration was selected to mimic the effluent of the WWTP located at Cranfield University, UK;

(2) A solution containing 14.74 mg NH_4^+/L and 28.89 mg Ca^{2+}/L, dissolved in DI water using NH_4Cl (purity stated >99%, Fisher Scientific, UK) and $CaCl_2$ (purity stated >99%, Fisher Scientific, UK);

(3) Tap water to analyse different cations concentrations with addition of NH_4^+ to mimic the effluent wastewater concentration the WWTP at Cranfield University, UK. Using tap water adds the presence of cations such as Ca^{+2}. Mg^{2+} and Na^+;

(4) Real effluent wastewater from the Cranfield University WWTP, taken as a 24h composite sample; and

(5) Real wastewater from a WWTP with 200,000 p.e. (not further described due to confidentiality requirements).

The characteristics of the different wastewaters analysed are presented in Table 1.

Table 1. Initial concentration of cations in experiments

	Exp 1	Exp 2	Exp 3	Exp 4	Exp 5
NH_4^+ (mg/l)	**12.74** ± 2.54	**14.74** ± 1.54	**10.56** ± 0.32	**12.00** ± 5.08	**32.8** ± 1.52
NH_4^+ (meq/l)	**0.91** ± 0.18	**1.05** ± 0.11	**0.75** ± 0.023	**0.86** ± 0.36	**2.34** ± 0.11
Ca^{2+} (mg/l)		**28.89** ± 7.82	**42.03** ± 0.89	**70.09** ± 8.49	**118.86** ± 1.15
Ca^{2+} (meq/l)		**1.44** ± 0.39	**2.1** ± 0.04	**3.50** ± 0.42	**5.9** ± 0.057
Mg^{2+} (mg/l)			**5.52** ± 0.02	**8.03** ± 1.84	**6.91** ± 0.47
Mg^{2+} (meq/l)			**0.45** ± 0.002	**0.67** ± 0.15	**0.58** ± 0.04
Na^+ (mg/l)			**36.14** ± 0.25	**85.82** ± 14.52	**105.9** ± 3.56
Na^+ (meq/l)			**1.57** ± 0.011	**3.73** ± 0.63	**4.60** ± 0.15
pH	**6.9** ± 0.2	**7.1** ± 0.2	**7.2** ± 0.1	**8.1** ± 0.1	**7.3** ± 0.1

The experiments were run for 6 hours and samples were taken every hour. Successively, the media

was regenerated for two hours using a brine containing 10%wt K^+ (purity stated >99%, Fisher Scientific, UK). Five different experiments with different number of regeneration cycles were carried out in order to analyse the performance of the zeolite under different conditions and calibrate the model: Exp. 1-2 (five cycles), Exp. 4 (three cycles), Exp. 3 and 5 (two cycles). The samples were mixed at 180 rpm on an orbital shaker (Stuart Orbital Shaker, Bibby Scientific Ltd., Staffordshire, UK).

The concentration of NH_4^+, K^+, Ca^{2+}, Mg^{2+} and Na^+ ions in the samples was measured using the Ion Chromatography DionexTM AS-DV Autosampler (Thermo scientific, https://www.thermofisher.com/order/catalog/product/068907).

2.2. Description of the mathematical model

The mathematical model was constructed following the guidelines given in the physico-chemical plant wide modelling (PC-PWM) methodology proposed by Ceit (Grau *et al.,* 2007; Lizarralde *et al.,* 2015). This methodology requires two steps: (1) the definition of the model components and transformations and (2) the mass transport definition for the unit process model.

2.2.1. Description of the model components and transformations

The mathematical model presented in this paper describes the mass balances that take place during the IEX using a stoichiometric matrix and the kinetic of the IEX process based on the selectivity of the media, the mass of media and environmental conditions.

The components included in the model are those measured during the experimental work and it considers the most common cations in wastewater: NH_4^+, Ca^{2+}, Mg^{2+}, Na^+ and K^+. The components consider the cations dissolved in wastewater (S) and the cations taken up by the media (q). The stoichiometry was described ensure mass and charge continuity, thus 1 equivalent of Ca^{2+} or Mg^{2+} was substituted by 2 equivalents of NH_4^+, Na^+, or K^+. For example, in transformation 1 (Table 2), 1 meq of NH_4^+ is removed from wastewater and it is exchanged with 1 meq of K^+, which is released to the bulk water. In addition to IEX processes, the possibility of K^+ released by the media was included

in reaction 21. The mass balances are compiled in the stoichiometric matrix presented in Table 2.

Table 2. Stoichiometric matrix for the description of the ion exchange process.

	SIN	SK	SCa	SMg	SNa	qNH4	qK	qCa	qMg	qNa
	g N	g K	g Ca	g Mg	g Na	g N	g K	g Ca	g Mg	g Na
1. NH4-K IEX	-1	$\frac{M_w(K)}{M_w(N)}$				+1	$-\frac{M_w(K)}{M_w(N)}$			
2. NH4-Ca IEX	-2		$\frac{M_w(Ca)}{M_w(N)}$			+2		$-\frac{M_w(Ca)}{M_w(N)}$		
3. NH4-Mg IEX	-2			$\frac{M_w(Mg)}{M_w(N)}$		+2			$-\frac{M_w(Mg)}{M_w(N)}$	
4. NH4-Na IEX	-1				$\frac{M_w(Na)}{M_w(N)}$	+1				$-\frac{M_w(Na)}{M_w(N)}$
5. Ca-K IEX		2	$-\frac{M_w(Ca)}{M_w(K)}$				-2	$\frac{M_w(Ca)}{M_w(K)}$		
6. Ca-NH4 IEX	2		$-\frac{M_w(Ca)}{M_w(N)}$			-2		$\frac{M_w(Ca)}{M_w(N)}$		
7. Ca-Mg IEX			$-\frac{M_w(Ca)}{M_w(Mg)}$	1				$\frac{M_w(Ca)}{M_w(Mg)}$	-1	
8. Ca-Na IEX			$-\frac{M_w(Ca)}{M_w(Na)}$		1			$\frac{M_w(Ca)}{M_w(Na)}$		-1
9. Mg-K IEX		2		$-\frac{M_w(Mg)}{M_w(K)}$			-2		$\frac{M_w(Mg)}{M_w(K)}$	
10. Mg-NH4 IEX	2			$-\frac{M_w(Mg)}{M_w(N)}$		-2			$\frac{M_w(Mg)}{M_w(N)}$	
11. Mg-Ca IEX			1	$-\frac{M_w(Mg)}{M_w(Ca)}$				-1	$\frac{M_w(Mg)}{M_w(Ca)}$	
12. Mg-Na IEX				$-\frac{M_w(Mg)}{M_w(Na)}$	2				$\frac{M_w(Mg)}{M_w(Na)}$	-2
13. Na-K IEX		$\frac{M_w(K)}{M_w(Na)}$			-1		$-\frac{M_w(K)}{M_w(Na)}$			1
14. Na-NH4 IEX	$\frac{M_w(N)}{M_w(Na)}$				-1	$-\frac{M_w(N)}{M_w(Na)}$				1

15. Na-Ca IEX			$\frac{M_w(Ca)}{M_w(Na)}$		-2			$-\frac{M_w(Ca)}{M_w(Na)}$		2
16. Na-Mg IEX				$\frac{M_w(Mg)}{M_w(Na)}$	-2				$-\frac{M_w(Mg)}{M_w(Na)}$	2
17. K-NH4 IEX	$\frac{M_w(N)}{M_w(K)}$	-1				$-\frac{M_w(N)}{M_w(K)}$	1			
18. K-Ca IEX		-2	$\frac{M_w(Ca)}{M_w(K)}$				2	$-\frac{M_w(Ca)}{M_w(K)}$		
19. K-Mg IEX		-2		$\frac{M_w(Mg)}{M_w(K)}$			2		$-\frac{M_w(Mg)}{M_w(K)}$	
20. K-Na IEX		-1			$\frac{M_w(Na)}{M_w(K)}$		1			$-\frac{M_w(Na)}{M_w(K)}$
21. K desorption		1					-1			

The process kinetics of the mathematical model considers the environmental conditions at which the process is happening. The kinetic model constructed in this paper was based on the kinetic expressions presented by Thomas (1944) and the simplified intraparticle diffusion model by Worch, (2012). The kinetic rate proposed for the ion-exchange processes (k) from 1 to can be expressed with following Equation 1 and 2:

$$\rho_k = k_{r,i-j} \cdot a_{VA} \cdot C_{w,i} \cdot (q_{max} \cdot M_w(i) \cdot m_{zeol} - q_i) \cdot \frac{q_j}{q_i + 0.001} \cdot V_w \quad \text{Eq. 1}$$

For reaction 21:

$$\rho_{21} = k_{r,K} \cdot a_{VA} \cdot q_K \cdot (C_{w,K} - C_{K,eq}) \cdot V_w \quad \text{Eq. 2}$$

Where,

- $k_{r,i-j}$ is the kinetic rate for the ion exchange process between the cation i (taken up by the media) and the cation j (released by the media);
- a_{VA} is the specific area of the media (m^2);
- $C_{w,i}$ is the bulk concentration of cation being taken up by the media (g/m^3);

193 - $C_{k,eq}$ is the equilibrium concentration of K^+ (g/m^3);

194 - q_{max} is the maximum exchange capacity of the media (meq/g);

195 - $M_w(i)$ is the molecular weight of cation i per meq (g/meq);

196 - m_{zeol} is the mass of media present in the system (g);

197 - q_i is the mass of cation i taken up by the media (g);

198 - q_j is the mass of cation j released by the media (g); and

199 - V_w is the volume of water present in the reactor (m^3).

200 - Term (qj/(qj+0,001) was included to guarantee simulation stability

201 The IEX process is described by means of ordinary differential equations (ODEs), defined with
202 stoichiometry and kinetics formulation. In addition to the IEX processes, chemical acid-base
203 equilibrium and complex ion pairing reactions were considered following the guidelines presented in
204 Lizarralde *et al.,* (2015). These equilibrium reactions are a set of fast processes described using
205 implicit, nonlinear algebraic equations (AEs). The chemical model is a tailor-made solution suited
206 for the components considered in the stoichiometric matrix.

207 2.2.2. Description of the unit process model

208 Two different phases were considered in the mathematical model: the aqueous phase (with the cations
209 to be removed) and the solid phase (with the cations to be exchanged). Consequently, two mass
210 balances were defined in the mathematical model to reproduce the behaviour of each phase and these
211 are formulated as follows:

212 Mass transport in the aqueous phase:

$$\frac{d\overline{MS}_w}{dt} = \bar{\dot{m}}_{w,in} - \bar{\dot{m}}_{w,out} + \bar{E}_w^T \cdot \bar{\rho}_w \qquad \text{Eq. 3}$$

213 Mass transport in the solid phase (onto media surface):

$$\frac{d\overline{M}_q}{dt} = \bar{E}_w^T \cdot \bar{\rho}_w \qquad \text{Eq. 4}$$

214 Where,

215 $\frac{d\overline{MS}_w}{dt}$ is the variation of mass of dissolved compounds in water;

216 $\bar{\dot{m}}_{w,in}$ is the inlet water and dissolved compound fluxes;

217 $\bar{\dot{m}}_{w,out}$ is the outlet water and dissolved compound fluxes;

218 $\bar{E}_w^T$ is the transpose of the stoichiometric matrix; and

219 $\bar{\rho}_w$ is the kinetic vector.

220 **2.3. Calibration of the mathematical model**

221 The experimental results were used to calibrate the mathematical model in order to find the optimum
222 kinetic parameters to reproduce the real behaviour of the ion exchange process described in section
223 2.1.

224 According to equations 1 to 20 (Table 2), the ion exchange process kinetics depended on the kinetic
225 parameter (k_{r,i_j}); the specific surface area of the zeolite (a_{VA}), the concentration of cations in the bulk
226 solution ($C_{w,i}$), the maximum concentration capacity (q_{max}), the mass of zeolite present in the
227 experiment (m_{zeol}), the amount of cations taken up by the media (q_i) and the volume of water (V_w).

228 The concentration of cations in the bulk solution and in the media are state variables and were
229 calculated from the integration of the model (i.e. model results). The volume of water and mass of
230 zeolite were determined by the experimental conditions, 1 L and 10 g in the experiments undertaken
231 in the laboratory. The specific surface was determined by the characteristics of the zeolite: the zeolite
232 is spherical with radius 2 mm, thus a_{VA} was $5 \cdot 10^{-5}$ (m^2) while the maximum CEC of the zeolite was
233 4.6 meq/g media (Canellas *et al.,* 2019a). The kinetic parameters were adjusted to minimize the error
234 between experimental results and the results predicted by the model.

235 For the calibration of the ion exchange process, Figure 1 shows the sequential parameter estimation
236 procedure that was followed. First, the parameters for the interaction between the NH_4^+ and K^+ in
237 reactions 1, 17 and 21 (Table 2) were calibrated using the experimental results obtained in the first
238 set of experiments, where only NH_4^+ was present in the water. The parameter adjustment was an

239 iterative procedure. Initially, all the parameters were considered to be 0. The $K_{r\_NH4\_K}$ was adjusted
240 in order to meet the NH_4^+ concentration at the end of the experimental cycle. Having that value
241 adjusted, the parameters $K_{r\_K\_Nh4}$ was estimated in order to mimic the shape of the NH_4^+ concentration
242 decrease. These values were changed iteratively until both, the final removal and evolution of NH_4^+
243 concentration were reproduced, minimizing the error between experimental and simulated data.
244 Finally, K_{r_k} was adjusted to reproduce the concentration of K^+.

245 Secondly, the interaction between the NH_4^+, Ca^{2+} and K^+ described in reactions 2, 5, 6 and 18 (Table
246 2) was calibrated with data from the second set of experiments adopting results from the first step.
247 The calibration was carried out following the procedure presented in Figure 1 and in a similar way to
248 Step 1. First the parameter $K_{r\_Ca\_K}$ was adjusted to fit the final Ca^{2+} removal and $K_{r\_K\_Ca}$ was adjusted
249 to fit the shape of the Ca^{2+} removal. Having these parameters adjusted the $K_{r\_NH4\_Ca}$ was adjusted to
250 meet the final NH_4^+ concentration and $K_{r\_Ca\_NH4}$ was adjusted to fit the shape and the final value of
251 the NH_4^+ concentration. Finally, the concentration of K^+ was evaluated. If the evolution was not
252 reproduced correctly, the parameters were adjusted. This process was done iteratively until the shape
253 and final concentrations of NH_4^+, Ca^{2+} and K^+ were reproduced correctly.

254 Thirdly, the calibration of the interactions between NH_4^+, Ca^{2+}, Na^+ and K^+ was calibrated with the
255 data set obtained in experiments 3. In the fourth step, the interactions between all cations NH_4^+, Ca^{2+},
256 Na^+, Mg^{2+} and K^+ were calibrated using data from Exp. 4. The procedure followed for the parameter
257 estimation in steps 3 and 4 is shown in Figure 1 and is analogous to steps 1 and 2

258 Finally, the calibrated parameters were used to simulate conditions in Experiment 5 and check the
259 model results. It must be noted that in order to estimate all the model parameters guaranteeing the
260 identifiability of all these parameters, all hourly data for all cations' concentrations, the evolution of
261 concentrations and final removal efficiency were considered.

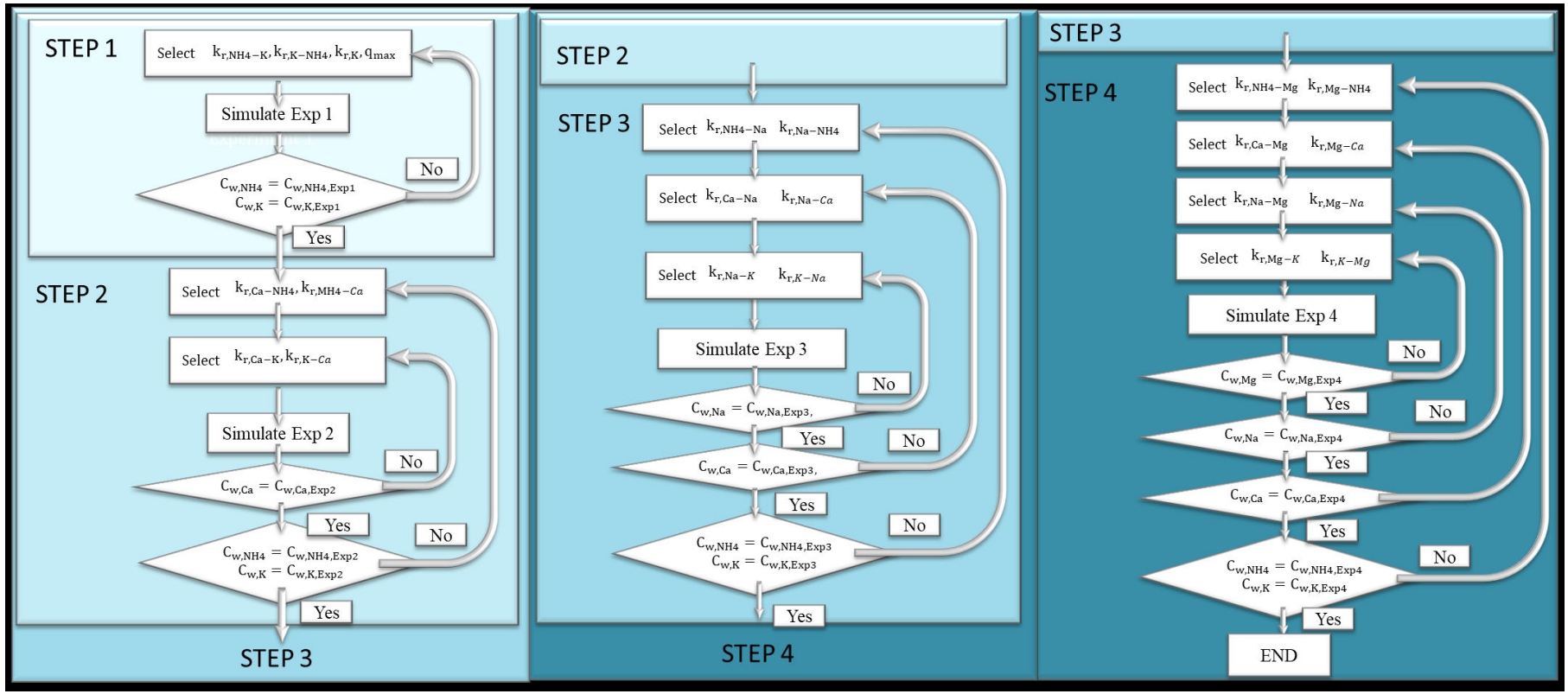

Figure 1. Parameter adjusting procedure

2.4. Experimental validation of the mathematical model

The mathematical model was validated by analysing the capacity of the model to reproduce an experimental breakthrough curve. The breakthrough curve shows the concentration of the cations removed in the bulk solution at the outlet of the ion exchange column in continuous operation. These curves are conventionally used to design and define the operational conditions of the columns. The model prediction was compared to experimental data available in Canellas *et al.,* (2019b) to show the potential of the model to mimic reality.

2.4. Exploration by simulation of the breakthrough curve of the zeolite for different operating conditions

Finally, the calibrated and validated model was used to carry out a scenario analysis to study the breakthrough curve of the zeolite for different operational conditions. The model was used to predict the modification of the breakthrough curve for different empty bed contact times (EBCT), influent cations concentrations and pH values.

3. RESULTS AND DISCUSSION

3.1. Experimental results

This section shows the results obtained in the experiments carried out. First, the evolution of the concentration in the bulk solution was analysed in order to study the kinetics of the IEX process. Secondly, the steady-state mass removed was analysed to discuss the competition between different cations. Finally, the release of K^+ and the correlation between the cations exchanged on the media surface was analysed.

3.1.1 Experimental evaluation of cation adsorption kinetics

The evolution of the concentration of the different cations in water was analysed by means of hourly sampling (Figure 2). The highest removal (>60%) was obtained during the first hour of the experiment while, in the following five hours, the removed rate declined and did not remove all the available cations. Analysis of the curves revealed that equilibrium was reached after four hours. These results are consistent with the previous work carried out on both synthetic and natural zeolites for ammonia removal (Thornton *et al.,* 2007; Weatherley and Miladinovic, 2004).

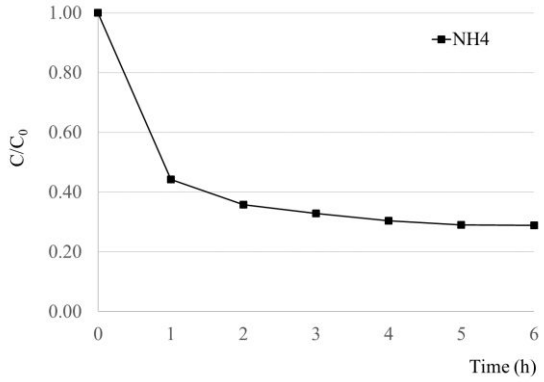

Exp. 1

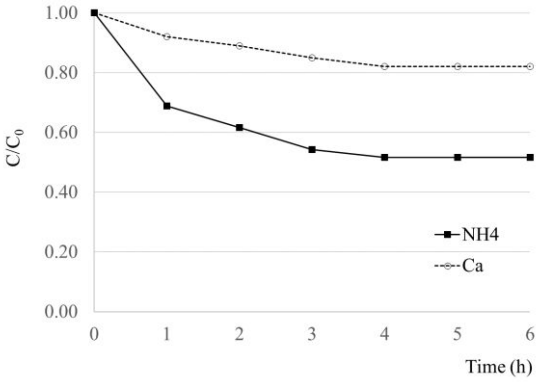

Exp. 2

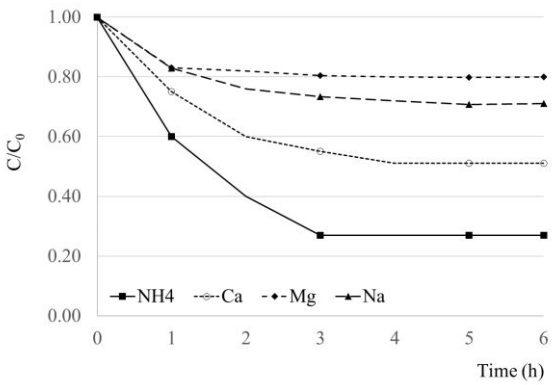

Exp. 3

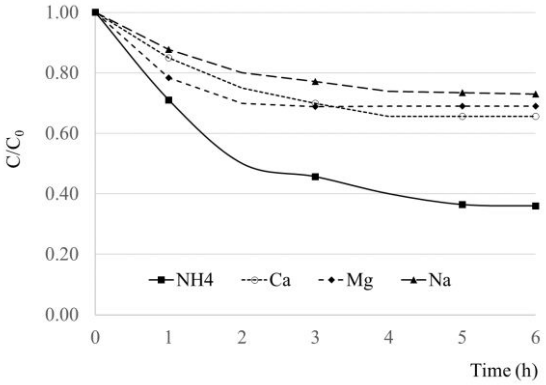

Exp. 4

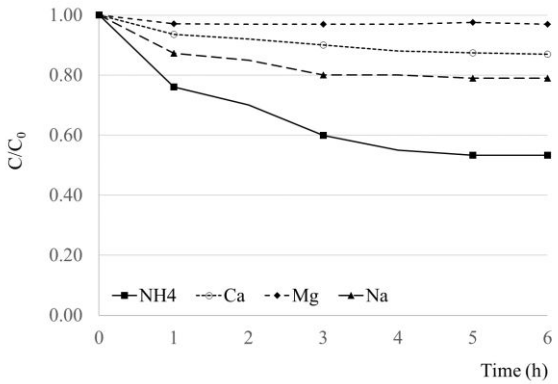

Exp. 5

Figure 2. Evolution in time of the C/C_o of different cations in all experiments (Exp. 1-5).

3.1.2. Experimental evaluation of cation adsorption capacity under competitive conditions

Once equilibrium was reached in all the experiments, the total cation exchange capacity of the zeolite (CEC) was analysed for the different concentrations of competing ions. Table 3 shows the average exchange capacity for the different ions in each experiment.

Table 3. Cations exchange capacity of the zeolite under steady state conditions

	Exp 1	Exp 2	Exp 3	Exp 4	Exp 5
NH_4^+ (meq/g zeol)	**0.065**±0.009	**0.051**±0.017	**0.055**±0.023	**0.054**±0.028	**0.110**±0.005
Ca^{2+} (meq/g zeol)		**0.026**±0.025	**0.102**±0.01	**0.121**±0.05	**0.075**±0.022
Mg^{2+} (meq/g zeol)			**0.009**±0.004	**0.008**±0.003	**0.001**±0.001
Na^+ (meq/g zeol)			**0.035**±0.008	**0.099**±0.02	**0.097**±0.006
Total (meq/g zeol)	**0.065** ± 0.009	**0.077** ± 0.023	**0.201** ± 0.081	**0.282** ± 0.071	**0.283**±0.034

The exchange of NH_4^+ varied in the different experiments depending on various factors. The average NH_4^+ exchange capacity in the first set of experiments for a single component in Exp. 1 was 0.065 meq/g (Table 3) which was consistent with previous investigations (Canellas *et al.,* 2019a; Guida *et al.,* 2020). The meq of NH_4^+ taken up by the media decreased by 21.5% in Exp. 2, 3 and 4 compared to Exp. 1 due to the impact on competing ions and was in accordance with previous works (Thornton *et al.,* 2007). In contrast, in Exp. 5, the NH_4^+ exchange capacity increased from 0.065 to 0.110 meq/g due to an increase in the initial NH_4^+ concentration. Previous studies have shown that the maximum NH_4^+ exchange capacity of the zeolite is 4.6 meq/g (Canellas *et al.,* 2019a).

The adsorption of Ca^{2+}, Mg^{2+} and Na^+ increased as the initial concentration of each cation increased. However, in Exp. 5 the adsorption of these cations decreased, even though their initial concentration increased and reflects the high adsorption of ammonia observed. Finally, the total cation equivalent exchange efficiency was analysed. This increased from 0.065 meq/g in Exp. 1 to 0.283 meq/g in Exp. 5. As the maximum NH_4^+ exchange capacity of this zeolite is 4.6 meq/g (Canellas *et al.,* 2019b), the media was far from being saturated in the experiments performed in the work presented in this paper.

3.1.3. Effect of the different conditions on CEC:K ratio

The K^+ concentration increased in time consistent with the uptake of the other ions. The shape of the

curve was similar to the removal efficiency; the release was high in the first hour and it declined in the following hours reaching equilibrium after 4 hours (Figure 3). The meq of K^+ released into the water was directly compared to the uptake of the other cations (NH_4^+, Ca^{2+}, Mg^{2+}, Na^+) to establish an experimental CEC: K ratio (Table 4). The ratio varied between 1:1.1 and 1:1.8 and compares to the theoretical CEC:K ratio of 1:1. The observed difference in CEC:K ratio indicates that there was a release of K^+ which were not exchanged with other cations present in the wastewater. This confirms the need to include reaction 21 in the mathematical model (Table 2).

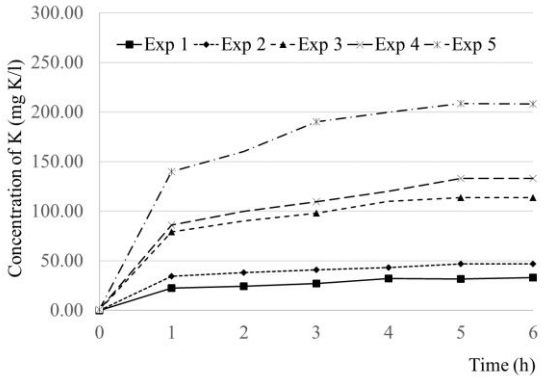

Figure 3. Evolution in time of the concentration of K^+ in the water in all experiments

Table 4. Amount of K^+ released during exchange process and CEC:K ratio

	Exp 1	Exp 2	Exp 3	Exp 4	Exp 5
K^+ released (meq/g zeol)	0.084	0.12	0.29	0.34	0.53
CEC:K	1:1.3	1:1.5	1:1.1	1:1.2	1:1.8

The results shown in this paper represent the average values in the different cycles undertaken in each set of experiments. Th capacity of the media was not reduced from one cycle to another, showing that the regeneration was effective under these conditions and the media was completely regenerated. The yield of zeolite was not decreased throughout the cycles, which showed that the regenerant used is valid for the four cations analysed.

3.2. Calibration of the mathematical model

The main results obtained in the calibration process are presented below.

STEP1: Calibration of the ammonia-potassium interaction

The first step of the calibration consisted of the adjustment of the kinetic constants in Eq. 1, Eq. 17 and Eq. 21 to fit the results in experiment 1 (Figure 1). Fourteen experimental points were available for the calibration of 3 kinetic parameters, consequently the model parameters were identifiable with the experimental data available. Table 5 shows the values adopted by the parameters that minimize the error.

Table 5. Calibrated value of the kinetic parameters ammonia-potassium interaction

Parameter	Value	Units
$K_{r\_NH4\_k}$	550	$m^{-2} \cdot g^{-2} \cdot s^{-1}$
$K_{r\_k\_NH4}$	70	$m^{-2} \cdot g^{-2} \cdot s^{-1}$
K_{r_K}	18	$m^{-2} \cdot g^{-2} \cdot s^{-1}$

Figure 4 shows the capability of the model to predict the behaviour of the experiments undertaken. The model was able to predict the evolution of the concentration of NH_4^+ in the aqueous phase, showing a sharp decrease in concentration in the first hour and slowing down in the following hours.

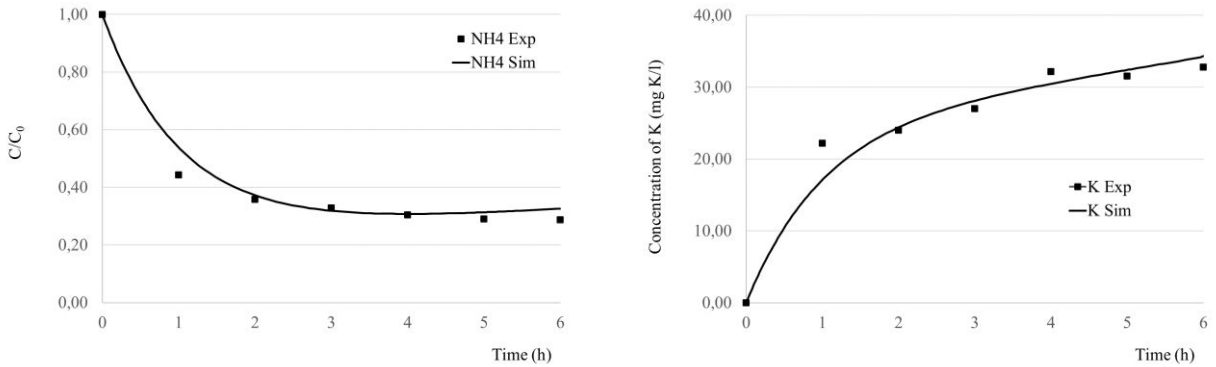

Figure 4. Comparison of the experimental and model results for the ammonia removal with no competing ions

STEP 2: Calibration of the ammonia-calcium-potassium interaction

Once the parameters for ammonia-potassium interactions were calibrated, the second set of experiments was used for the calibration of equations of reactions 2, 5, 6 and 18 (Table 2). The values

351 for the adjusted parameters in the Step 2 are presented in Table 6.

352 **Table 6.** Calibrated value of the kinetic parameters for calcium-potassium interaction

Parameter	Value	Units
Kr_Ca_K	10	$m^{-2} \cdot g^{-2} \cdot s^{-1}$
Kr_K_Ca	23	$m^{-2} \cdot g^{-2} \cdot s^{-1}$
Kr_NH4_Ca	0	$m^{-2} \cdot g^{-2} \cdot s^{-1}$
Kr_Ca_NH4	10	$m^{-2} \cdot g^{-2} \cdot s^{-1}$

353 Figure 5 shows the capability of the model to predict the behaviour of the experiments undertaken.
354 The model was able to reproduce the removal of NH_4^+ and Ca^{2+}. In the case of NH_4^+, the model
355 estimated a slightly higher removal than in the experiments, whereas, in the case of Ca^{2+}, the model
356 was able to reproduce the performance during the six hours of experiments. In addition, the release
357 of K^+ was reproduced correctly by the model.

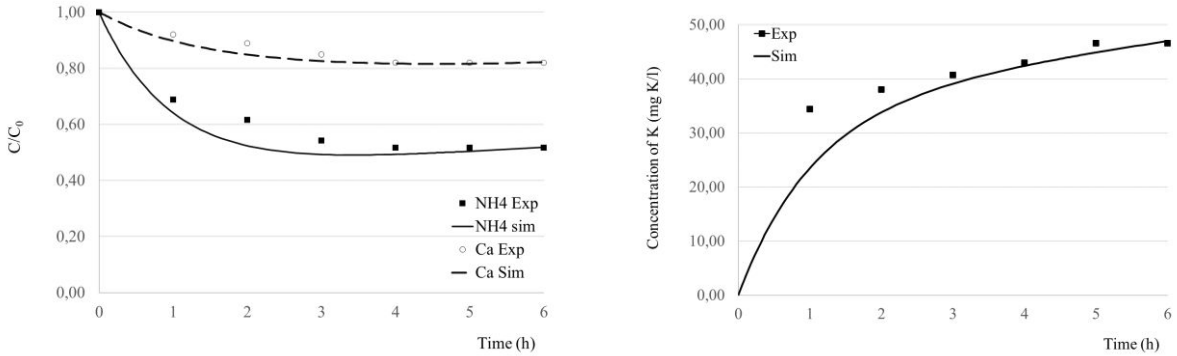

358 **Figure 5.** Comparison of the experimental and model results for the ammonia removal with calcium as a competing ion
359 STEP 3: Calibration of the ammonia-calcium-sodium-magnesium-potassium interaction

360 Next the calibration of the ammonia-calcium-sodium-magnesium-potassium interaction parameters
361 was completed. Table 7 shows the values of the calibrated kinetic parameters while Figure 6 shows
362 the capability of the model to predict the behaviour of the experiments undertaken.

363 **Table 7.** Calibrated values of the ammonia-calcium-sodium-potassium interactions

Parameter	Value	Units
Kr_NH4_Na	135	$m^{-2} \cdot g^{-2} \cdot s^{-1}$
Kr_Ca_Na	17	$m^{-2} \cdot g^{-2} \cdot s^{-1}$

Kr_Na_NH4	0	$m^{-2} \cdot g^{-2} \cdot s^{-1}$
Kr_Na_Ca	5	$m^{-2} \cdot g^{-2} \cdot s^{-1}$
Kr_Na_Mg	0	$m^{-2} \cdot g^{-2} \cdot s^{-1}$
Kr_Na_K	300	$m^{-2} \cdot g^{-2} \cdot s^{-1}$
Kr_K_Na	15	$m^{-2} \cdot g^{-2} \cdot s^{-1}$
Kr_NH4_Mg	0	$m^{-2} \cdot g^{-2} \cdot s^{-1}$
Kr_Ca_Mg	0	$m^{-2} \cdot g^{-2} \cdot s^{-1}$
Kr_Mg_NH4	0	$m^{-2} \cdot g^{-2} \cdot s^{-1}$
Kr_Mg_Ca	0	$m^{-2} \cdot g^{-2} \cdot s^{-1}$
Kr_Mg_Na	0	$m^{-2} \cdot g^{-2} \cdot s^{-1}$
Kr_Mg_K	70	$m^{-2} \cdot g^{-2} \cdot s^{-1}$
Kr_Na_Mg	0	$m^{-2} \cdot g^{-2} \cdot s^{-1}$
Kr_K_Mg	2	$m^{-2} \cdot g^{-2} \cdot s^{-1}$

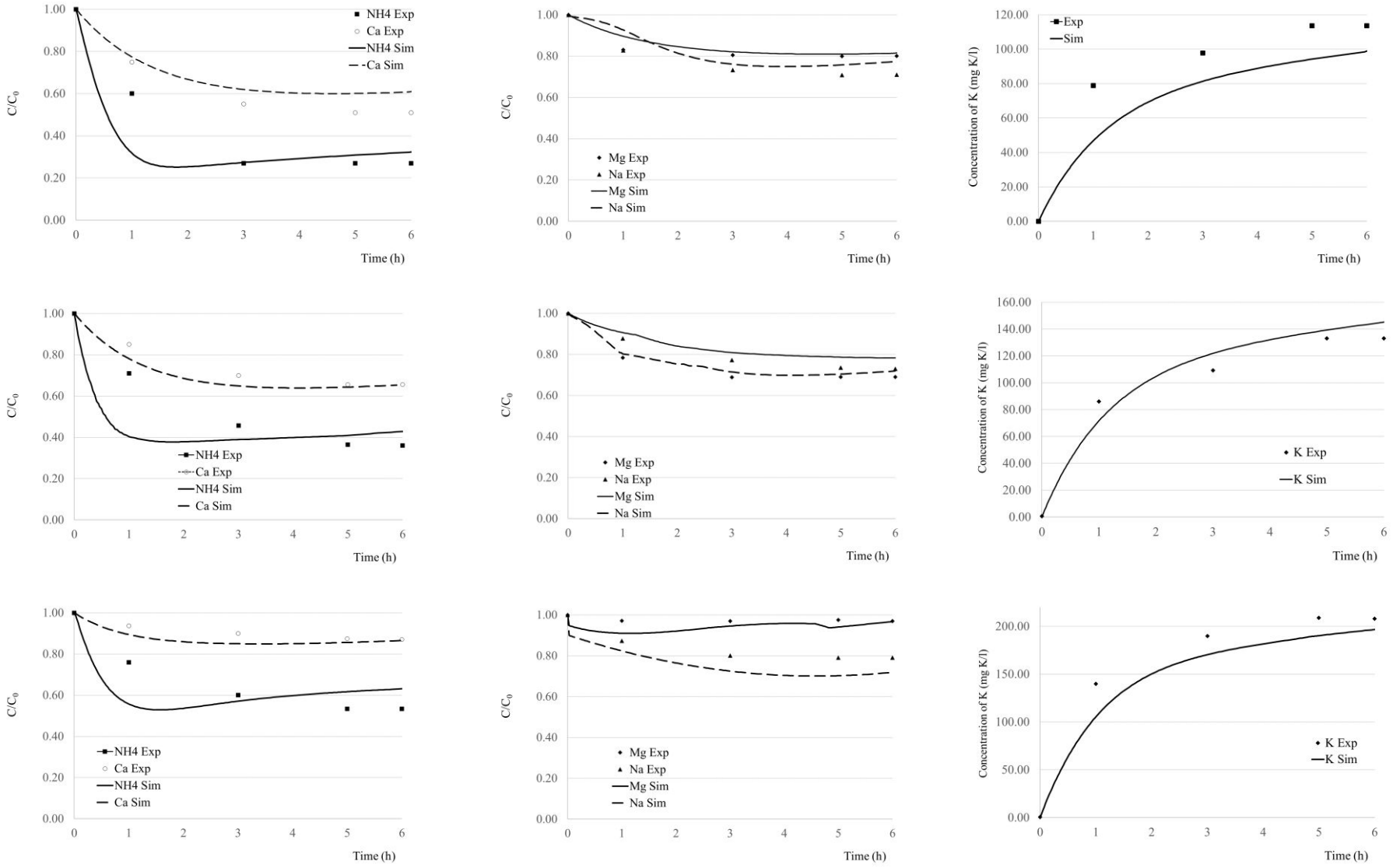

365 **Figure 6.** Comparison of the experimental and model results for the ammonia removal with the considered competing ions

366

As in the case of experiment Exp. 2, the model predicted a higher removal of NH_4^+ in the first hour, however, the removal predicted in hours 3, 4 and 5 corresponded to the removal observed experimentally. The removal of Ca^{2+} and Mg^{2+} was correctly predicted by the model for all the experiments as well as the removal of Na^+ for Exp. 3 and 4. However, a slightly higher removal was predicted by the model in Exp 5 where the initial concentration of Na^+ is the highest, which could have caused the slight difference between experimental and simulated data. Finally, the evolution of K^+ was reproduced by the model in all the experiments.

Once the model was calibrated, a comparison between the experimental and model results was performed (Figure 7) and the model was able to reproduce the experimental data correctly.

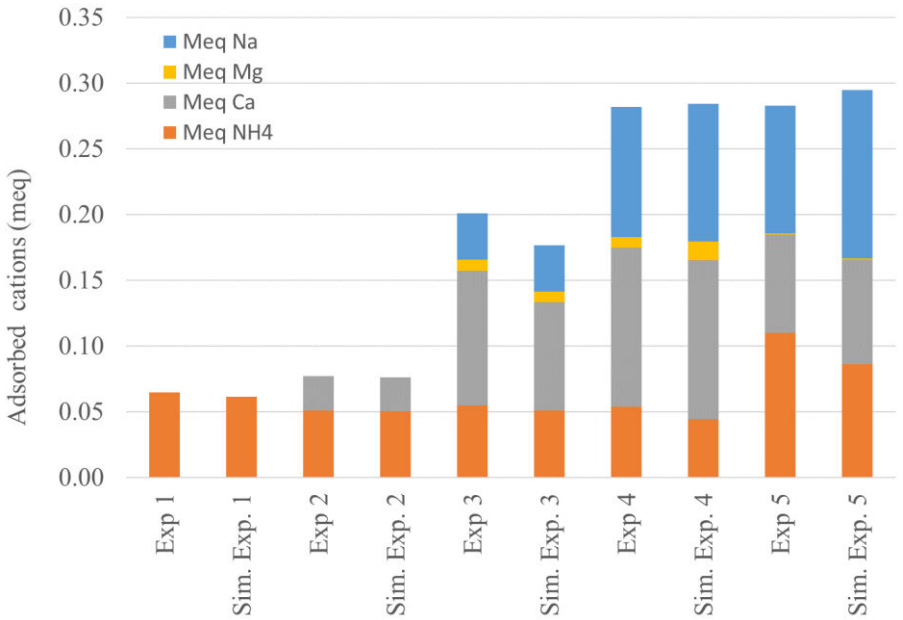

Figure 7. Comparison of model results and experimental result under steady-state conditions

3.2.1. Analysis of the errors

Figure 8 (left) shows the comparison of the experimental and simulated data. The two points outside the confidence interval correspond to the prediction of NH_4^+ concentration in the first hour in experiments Exp 1 and Exp 2. However, 64 points, 97% of total compared data, are within the dashed lines showing a good representation of the experimental data.

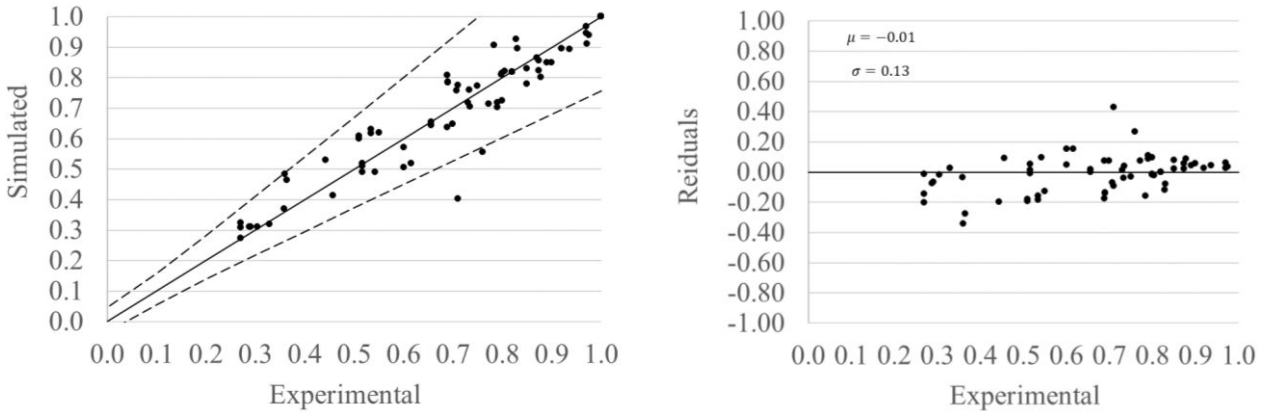

Figure 8. Comparison of experimental and simulated data (Left). The black line represents the linear regression of both sets of data and the dashed lines represent the confidence interval of 95% for the linear regression. Residuals of experimental and simulated data (Right)

Figure 8 (right) represents the residuals of the simulated data. The mean value of the residuals was -0.01 with a standard deviation of 0.13. These results showed that the model was able to reproduce the real behaviour of the process under the conditions analysed experimentally.

3.3. Validation of the mathematical model to reproduce breakthrough curves

This section shows the performance of the mathematical model for the description of the continuous operation of the ion-exchange process following the experimental conditions employed by Canellas *et al.,* (2019a), where 76.84 g of zeolite with size ranging between 1 and 1.7 mm were used to treat the wastewater. The media bed volume was 100 mL, the flow rate treated was 12.5 ml/min, resulting in an EBCT of 8 minutes. In this first analysis of the continuous operation, synthetic water with 5 mg N/l of NH_4^+ was used.

Using the mathematical model calibrated in the previous section a simulation was run and the simulation results compared to experimental results are shown in Figure 9.

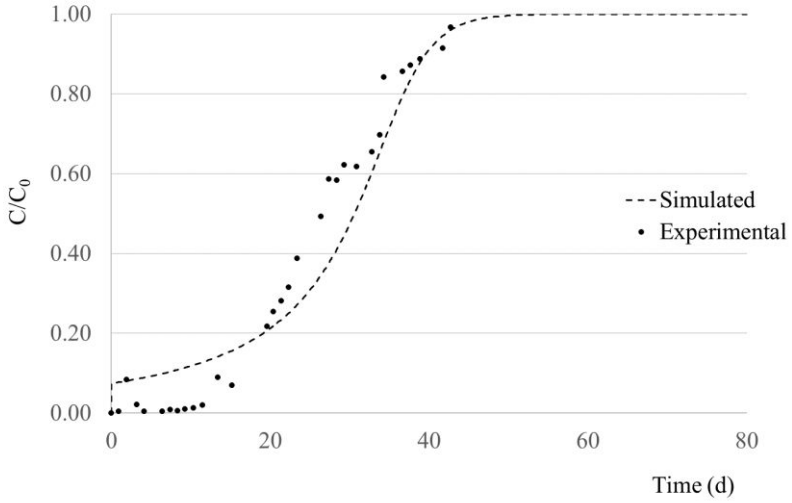

Figure 9. Comparison the experimental and simulated breakthrough curves

The breakthrough curve predicted by the model shows the evolution of the concentration of NH_4^+ in time and it was adjusted to the real performance (Canellas *et al.,* 2019b). Figure 9 shows that, in the first 20 days, the ratio C/C_o was below 0.2 showing a good NH_4^+ removal. Successively, the media started to get saturated and the C/C_o ratio increased until it reached saturation point in day 40. At this point, the media was not able to remove any more NH_4^+: the value of the C/C_o ratio is 1 showing that all the NH_4^+ entering the column leaved the column. Having this breakthrough curve permits the definition of the optimum cycle of uptake-regeneration cycle duration. If a concentration of 2 mg/l is required in the effluent, the C/C_o ratio has to be 0.4, which was achieved for 30 days of operation under the defined operating conditions.

Having proven the capability of the model to predict the behaviour of the ion exchange process under continuous operating conditions, the following sections show the usefulness of the model to analyse different scenarios.

3.3. Exploration by simulation of the effect of different operational conditions on the breakthrough curve

3.3.1. Prediction of breakthrough curves for different EBCT

The impact of EBCT on cycle time revealed a significant decrease in cycle time as the eBCT was reduced (Figure 10). For instance, when increasing the EBCT form 2.5 minutes to 15 minutes, the

operating time to reach the saturation increased from 12 to 70 days. The limit for the C/C_o ratio of 0.4 was reached in 6.5 days when working at an EBCT of 2.5 minutes and in 50 days with EBCT of 15 minutes.

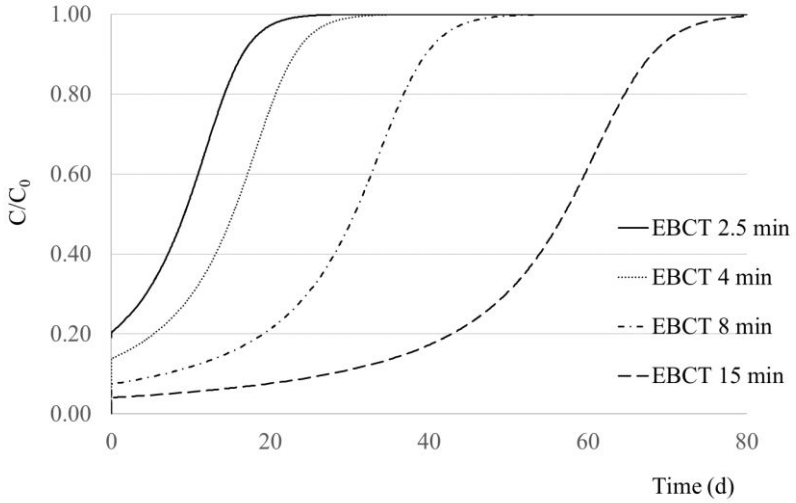

Figure 10. Effect of EBCT on the breakthrough curve

3.3.2. Prediction of breakthrough curves for different initial NH_4^+ concentrations

Increasing the influent NH_4^+ concentrations shifted the breakthrough curve to the left-hand side and thus reduce the cycle durations (Figure 11). The saturation of zeolite was achieved after 10 days of operation when treating wastewater with 30 mg NH_4^+/L of concentration of NH_4^+, whereas the saturation was reached after 40 days of operation when the initial concentration was 5 mg NH_4^+/L of NH_4^+. If a concentration of 2 mg NH_4^+/L is required in the effluent, this value was reached after 30 days, 13 days, 3.5 days and 1.5 days for influent concentrations of 5, 10, 20 and 30 mg NH_4^+/L, respectively.

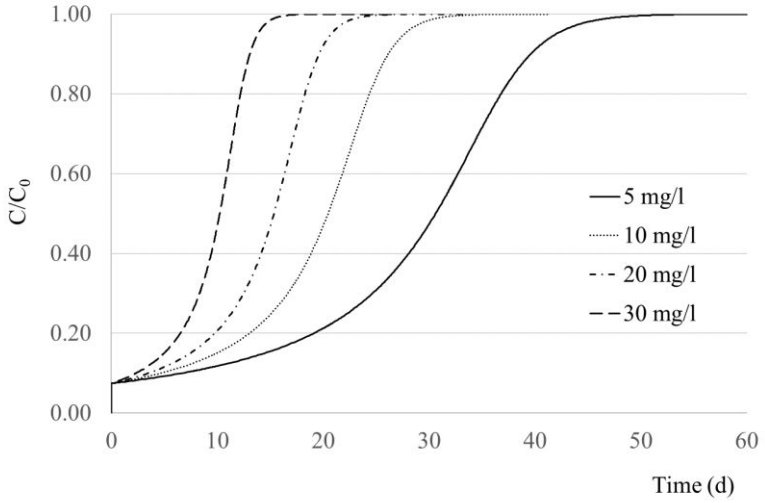

436 **Figure 11.** Effect of influent concentration on the breakthrough curve

437

438 **3.3.3. Effect of pH on different**

439 The efficiency of the ion exchange process depends on the value of the pH as this affects the
440 speciation of NH_4^+ (Leyva *et al.,* 2010). In this work, the breakthrough curve for different influent
441 pH values was examined theoretically using the mathematical model constructed. The baseline
442 scenario analysed in the previous sections had an influent pH of 7.2. In this analysis, pH values of
443 8.2, 9 and 9.7 were studied (Figure 12).

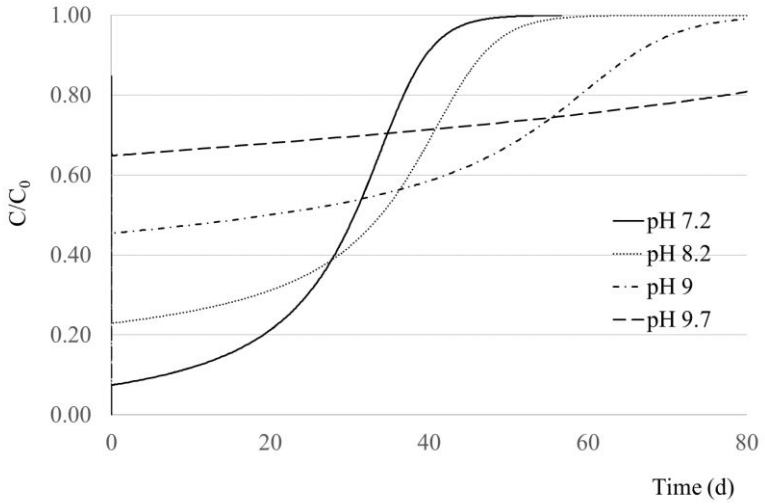

444 **Figure 12.** Effect of influent concentration on the breakthrough curve

445 At pH 7.2, all the NH_4^+ nitrogen is NH_4^+, thus it was removed correctly. At pH 8.2, part of the NH_4^+

446 exists in the form of NH_3 but only the fraction in the NH_4^+ form can be removed. In this case, the
447 limit of 2 mg NH_4^+/L was achieved after around 30 days, which was similar to the pH 7.2 value.
448 However, when analysing pH values higher than 9, the limit of 2 mg NH_4^+/L was not met. This was
449 caused by the fact that the majority of NH_4^+ is present in the gaseous form NH_3.

450 **3.3.4. Breakthrough curve for different cation concentrations**

451 The presence of competing ions has been proven to be crucial for the removal of ammonia when using
452 ion exchange technology. In this work, the NH_4^+ breakthrough curves were analysed for the different
453 wastewaters. Exp. 5 was included in the study due to the considerably higher initial concentration
454 compared to the other experiments which would affect the curve.

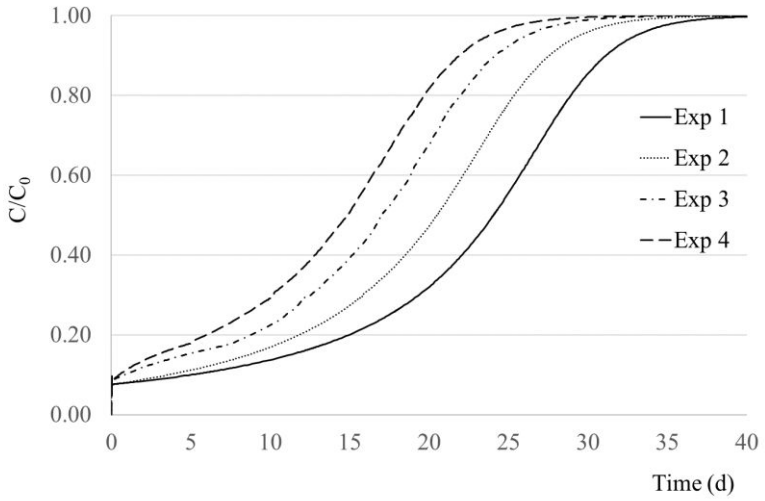

455 **Figure 13.** Effect of concentration of competing cations on the breakthrough curve

456 Figure 13 shows how different competing ions affect the NH_4^+ breakthrough curve. The limit of 2
457 NH_4^+/L in the effluent was achieved in day 11 for the first experiment where no competing ions were
458 present. The cycle time was reduced to 2.8 days when treating the real effluent of the wastewater
459 treatment plant (exp 4).

460 Having a continuous operation for different cases is time and resource consuming so the mathematical
461 model constructed in this paper is very useful to find optimum cycle durations. This exploration by
462 simulation study shows the potential of the mathematical model to analyse the effect of different
463 operational conditions on the ion exchange technology as well as the possibility of estimating the

optimum operating strategies for different wastewater characteristics

5. CONCLUSIONS

A new mathematical model able to describe the ion exchange for NH_4^+ removal and recovery in presence of competing ions has been developed and calibrated. The mathematical model has been proven to be able to reproduce the performance of the IEX process under different empty bed contact times, influent loads, pH and concentrations of competing ions.

The competition between different cations in water showed that, for a comparable initial concentration of NH_4^+, the presence of competing ions reduced the NH_4^+ exchange capacity by around 21%. During the ion exchange process the CEC:K ratio should be 1:1, however, the experimental analysis carried out in this study has shown a ratio between 1:1.2 and 1:1.8 indicating an additional loss of K^+.

The model has been used to explore the impact of key design and operating factors. This has revealed that prolonged operating cycles of 70 days can be achieved when using EBCTs of 15 minutes. However, this is very dependent on the influent NH_4^+ which reduces the cycle time as the concentration increases and the pH extends beyond pH 7. Above pH 9, the media does not remove NH_4^+, since all the NH_4^+ nitrogen is in the uncharged NH_3 form. Finally, it was seen that in presence of competing ions, the frequency of the regeneration has to be higher, reducing cycle duration.

The study by simulation has shown the potential of the mathematical model to reproduce the behaviour of the IEX process under different operating conditions and enable optimised designs to be developed.

ACKNOWLEDGMENT

This project has received funding from the Europe Union's Horizon 2020 research and innovation programme under grant agreement No 690323. I. Lizarralde would like to thank the Spanish Education and Culture ministry for the Mobility Grant "José Castillejo" (CAS19/00117). Finally, the

490 authors would like to thank the Spanish Education and Culture ministry for the Modyphos project
491 (PID2019-108378RB-I00).

492 **REFERENCES**

493 Batstone D.J and Keller J. (2002). Anaerobic digestion model No 1 (ADM1). Scientific and Technical
494 Report No 13. IWA Publishing, London.

495 Canellas, J., Soares, A., Jefferson, B., 2019a. Removing ammonia from wastewater using natural and
496 synthetic seolites: A batch experiment. https://doi.org/10.26434/chemrxiv.9831542.v1

497 Canellas, J., Soares, A., Jefferson, B., 2019b. A Comparison of natural and synthetic zeolites in
498 continuous column-based experiments for removing ammonia from wastewater.
499 https://doi.org/10.26434/chemrxiv.9857615.v1

500 Comstock, S. E. H. and Boyer, T.H. (2014). Combined magnetic ion exchange and cation exchange
501 for removal of DOC and hardness. Chemical Engineering Journal. 241, 366-375.

502 Ding, Y., and Sartaj, M. (2015). "Statistical analysis and optimization of ammonia removal from
503 aqueous solution by zeolite using factorial design and response surface methodology." Journal
504 of Environmental Chemical Engineering, 3(2), 807–814.

505 Flodman, H.R. and Dvorak, B. I. (2012). Brine reuse in ion-exchange softening: salt discharge,
506 hardness leakage and capacity tradeoffs. Water Environ. Res., 84 (2012), pp. 535-543

507 Grau P., de Gracia M., Vanrolleghem P.A. and Ayesa E. (2007). A new plant-wide modelling
508 methodology for WWTPs. Wat. Res. 41, 4357-4372.

509 Guida, S., Potter, C., Jefferson, B. and Soares, A. (2020). Preparation and evaluation of zeolites for
510 ammonium removal from municipal wastewater through ion exchange process. Scientific
511 Reports (10).

512 Guida, S., Van Peteghem, L., Lugmani, B., Sakarika, M., McLeod, A. McAdam, E.J., Jefferson, B.,
513 Rabaey, K., and Soares, A. (2022). Ammonia recovery from brines originating from a municipal
514 wastewater ion exchange process and valorization of recovered nitrogen into microbial protein.
515 Chemical Engineering Journal. 427. Henze, M., Gujer, W., Mino, T., and Van Loosdrecht, M.

516 C. M (2000). Activated Sludge Models ASM1, ASM2, ASM2d and ASM3. Scientific and
517 Technical Report No 9. IWA Publishing, London.
518 Henze, M., van Loosdrecht, M. C. M., Ekama, G. A. and Brdhanovic, D. (2008). Biological
519 Wastewater Treatment: Principles, Modelling and Design. IWA Publishing.
520 Huang, X., Guida, S., Jefferson, B. and Soares, A. (2020). Economic evaluation of ion-exchange
521 processes for nutrient removal and recovery from municipal wastewater. Clean Water. 3.
522 Iddya, A., Hou, D., Khor, C.M., Ren, Z., Tester, J., Pormanik, R., Gross, A. and Jassby, D. (2020).
523 Efficient ammonia recovery from wastewater using electrically conducting gas stripping
524 membranes. Environmental Science: Nano. 6.
525 Kumar, P., Pournara, A., Kim, K.H., Bansal, V, Rapti, S. and Manos, M. J. (2017). Metal-organic
526 frameworks: Challenges and opportunities for ion-exchange/sorption applications. Progress in
527 Materials Science. 86, 25-74.
528 Leyva-Ramos, R., Monsivais-Rocha, J. E., Aragon-Piña, A., Berber-Mendoza, M.S., Guerrero-
529 Coronado, R. M., Alonso-Dávila, P. and Mendoza-Barron (2010). Removal of ammonium from
530 aqueous solution by ion Exchange on natural and modified chabazite. Journal of Environmental
531 Mangemnt 91(12), 2662-2668.
532 Levchuk, I., Rueda Marquez, J. J. and Sillanpää, M. (2018). Removal of natural organic matter
533 (NOM) from water by ion exchange – A review. Chemosphere, 192, 90-104.
534 Lizarralde I., Fernández-Arévalo T., Brouckaert C. J., Vanrolleghem P. A., Ikumi D. S., Ekama G.
535 A., Ayesa E. and Grau P. (2015) A new general methodology for incorporating physico-
536 chemical transformations into multi-phase wastewater treatment process models. Water
537 Research (74) 239-256.
538 Olsson G. (2013). Water and Energy: Threats and Opportunities. IWA Publishing, London UK.
539 Prelot B., Araïssi M., Gras P., Marchandeau F. and Zajac J. (2018). Contribution of calorimetry to
540 the understanding of competitive adsorption of calcium, strontium, barium, and cadmium onto

4A type zeolite from two-metal aqueous solutions. Thermochimica Acta, 664, 39-47.

Robles, A., Aguado, D., Barat, R., Borrás, L., Bouzas, A., Bautista Giménez, J., Martí, N., Ribes, J., Ruano, M. V., Serralta, J., Ferrer, J. and Seco, A. (2020). New frontiers from removal to recycling of nitrogen and phophorus from wastewater in Circular Economy. Bioresource Technology. 300.122673.

Sancho, I., Licon, E., Valderrama, C., de Arespacochaga, N., López-Palau, S. and Cortina, J. L. (2017). Recovery of ammonia from domestic wastewater effluents as liquid fertilizers by integration of natural zeolites and hollow fibre membrane contactors. The Science of the Total Environment. 584-585:244-251.

Soares, A. (2020). Wastewater treatment in 2050: Challenges ahead and future vision in a European context. Environmental Science and Ecotechnology. 2 (2020) 100030.

Tchobanoglous, G., Burton, F. L. and Stensel H. D (2003). Wastewater Engineering, Treatment, Disposal, and Reuse (4th edition), McGraw-Hill, New York, NY

Thomas, H. C. (1944). Heterogeneous Ion Exchange in a Flowing System. Am. Chem. Soc. 1944, 66, 10, 1664–1666

Thornton, A., Pearce, P. and Parsons, S. A. (2007). Ammonium removal from liquid solution using ion exchange on to MesoLite, an equilibrium study. Journal of Hazardous Materials 147 (2007) 883-889.

Trgo, M., Medvidovic, N.V and Peric, J. (2011). Application of mathematical empirical models to dynamic removal of lead on natural zeolite clinoptilolite in a fixed bed column. Indian Journal of Chemical Technology. 18 (2): 123-131

Víctor-Ortega, M. D., Ochando-Pulido, J. M. and Martínez-Ferez, A. (2016). Performance and modeling of continuous ion Exchange processes for phenols recovery from olive mil wastewater. Process safety and Environmental Protection 100, 242-251.

Wang, Y., Liu, S., Xu, Z., Han, T., Chuan, S. and Zhu, T. (2006). Journal of Hazardous Materials

566 B136 (2006) 735-740.
567 Weatherley, L. R. and Miladinovic, N.D. (2004). Comparison of the ion exchange uptake of
568 ammonium ion onto New Zealand clinoptilolite and mordenite. Water Research, 28 (20) 4305-
569 12.
570 Worch, E. (2008). Fixed-bed adsorption in drinking water treatment: a critical review on models and
571 parameter estimation. J. Water Supply Res. T –AQUA. 57: 171-183.
572 Worch, E. (2012). Adsorption Technology in Water Treatment. De Gruyter.

2021-10-20

Development and calibration of a new mathematical model for the description of an ion-exchange process for ammonia removal in the presence of competing ions

Lizarralde, Izaro

Elsevier

Lizarralde I, Guida S, Canellas J, et al., (2021) Development and calibration of a new mathematical model for the description of an ion-exchange process for ammonia removal in the presence of competing ions. Water Research, Volume 206, November 2021, Article number 117779 https://doi.org/10.1016/j.watres.2021.117779